

# Parity-time symmetric holographic principle

Xingrui Song<sup>1</sup> and Kater Murch<sup>1</sup>

<sup>1</sup>*Department of Physics, Washington University, St. Louis, Missouri 63130, USA*

(Dated: October 5, 2022)

Originating from the Hamiltonian of a single qubit system, the phenomenon of the avoided level crossing is ubiquitous in multiple branches of physics, including the Landau-Zener transition in atomic, molecular and optical physics, the band structure of condensed matter physics and the dispersion relation of relativistic quantum physics. We revisit this fundamental phenomenon in the simple example of a spinless relativistic quantum particle traveling in (1+1)-dimensional space-time and establish its relation to a spin-1/2 system evolving under a  $\mathcal{PT}$ -symmetric Hamiltonian. This relation allows us to simulate 1-dimensional eigenvalue problems with a single qubit. Generalizing this relation to the eigenenergy problem of a bulk system with  $N$  spatial dimensions reveals that its eigenvalue problem can be mapped onto the time evolution of the edge state with  $(N - 1)$  spatial dimensions governed by a non-Hermitian Hamiltonian. In other words, the bulk eigenenergy state is encoded in the edge state as a hologram, which can be decoded by the propagation of the edge state in the temporal dimension. We argue that the evolution will be  $\mathcal{PT}$ -symmetric as long as the bulk system admits parity symmetry. Our work finds the application of  $\mathcal{PT}$ -symmetric and non-Hermitian physics in quantum simulation and provides insights into the fundamental symmetries.

In the 1980s, Richard Feynman envisioned the advantage of using quantum mechanical systems to simulate quantum physics [1]. As most formulations of quantum mechanics consider the systems to be governed by Hermitian Hamiltonians, the community established the theory of quantum computation based on combinations of unitary gate operations [2–5]. However, after decades of effort toward implementing quantum computers, we realize that even the most highly controlled quantum systems are open quantum systems [6–8]. These open quantum systems are non-unitary, suffering from the residual coupling with the environment causing dissipation and decoherence. In contrast to the stereotype that such non-unitary effects of evolution are always harmful, dissipation is now considered an important resource for quantum technologies, with extensive applications in quantum control, sensing, and simulation [9–17]. In this letter, we extend Feynman’s logic by taking advantage of open quantum systems as an efficient resource for quantum simulation. In particular, we show how the open quantum system evolution described by a non-Hermitian Hamiltonian [15, 18–30] allows one to map the eigenvalue problem of a 1-dimensional Hermitian system onto the time evolution of a qubit. Extending this reasoning suggests that an  $N$ -dimensional Hermitian bulk system can be mapped onto the non-Hermitian time evolution of a  $(N - 1)$ -dimensional edge system. In parallel with the research highlighting the bulk-boundary correspondence of non-Hermitian systems [31–35], our work finds the new application of these concepts to reduce the quantum resources required for encoding the spatial degrees of freedom in quantum simulation for Hermitian systems. We present two specific examples that illustrate the power of this concept: First, we propose an experimental scheme exploiting this relationship to perform quantum simulation of a scattering problem with reduced

quantum resources. Second, we examine the system of a Kitaev chain and show how the non-Hermitian evolution can model the physics of Majorana zero modes in one of the simplest topologically nontrivial models [36–40]. After demonstrating our method with two examples, we discuss the relation between Parity symmetry and Parity-Time ( $\mathcal{PT}$ )-symmetry and generalize the result to show how  $\mathcal{PT}$ -symmetric evolution of the edge state generates the solution of the eigenvalue problem of a bulk Hermitian system.

*The eigenvalue problem and  $\mathcal{PT}$ -symmetric evolution*—We start by considering the simple case of a massless Fermion moving in one dimension, which has a linear dispersion relation as shown in Fig. 1(a). The right and left moving particles form a two-state system  $\{|L\rangle, |R\rangle\}$ , which can be mapped onto a qubit. In this gapless limit, the Dirac equation is uncoupled. Once the two components are coupled, the particle acquires a mass resulting in an avoided crossing (Fig. 1(b)). In this case, the particle at rest is given by an equal superposition of the states  $|L\rangle$  and  $|R\rangle$ . In general, the state of a traveling particle is given by some linear combination of  $|L\rangle$  and  $|R\rangle$ . Particularly, the state  $|\pm\rangle = \frac{1}{\sqrt{2}}(|L\rangle \pm |R\rangle)$  represents the particle at rest with eigenenergy equal to  $\pm m$ . This picture implicitly incorporates the idea of separation of variables, where we downgrade the momentum from an operator to a parameter  $-i\partial_x \rightarrow k$ . Hence we can write the corresponding Schrödinger equation for the particle with the time coordinate treated as the independent variable,

$$i\partial_t \begin{pmatrix} \psi_L \\ \psi_R \end{pmatrix} = \begin{pmatrix} -k & m \\ m & k \end{pmatrix} \begin{pmatrix} \psi_L \\ \psi_R \end{pmatrix} = H(k) \begin{pmatrix} \psi_L \\ \psi_R \end{pmatrix}, \quad (1)$$

where we have set  $\hbar = c = 1$  for simplicity. This approach, however, is not the only option, and may not be the most convenient approach under some circumstances. Indeed, the Dirac equation does not prefer a specific time

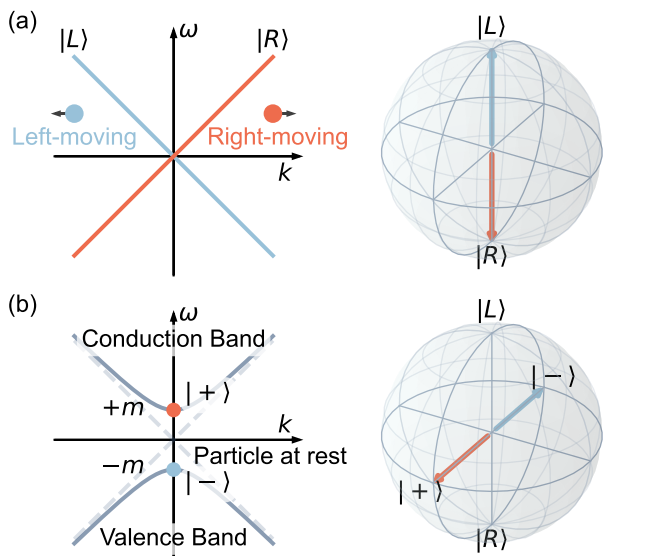


FIG. 1. **Dispersion relation, avoided crossings, and qubits.** (a) The linear dispersion relation of the left-moving and right-moving massless Fermions. These two states are labeled by  $|L\rangle$  and  $|R\rangle$ , respectively. They can be mapped onto a qubit, represented north and south pole on a Bloch sphere. (b) The dispersion relation of massive Dirac Fermion. Once the coupling is introduced, the dispersion relation exhibits an avoided crossing. The two states represent the particle at rest with  $\pm m$  eigenenergy are represented on the Bloch sphere along the  $\pm X$  axis.

or spatial coordinate.

Instead, we consider replacing the energy,  $\omega$  with a parameter and treat the spatial coordinate as the independent variable,

$$i\partial_x \begin{pmatrix} \psi_L \\ \psi_R \end{pmatrix} = \begin{pmatrix} \omega & -m \\ m & -\omega \end{pmatrix} \begin{pmatrix} \psi_L \\ \psi_R \end{pmatrix} = H_{\text{eff}}(\omega) \begin{pmatrix} \psi_L \\ \psi_R \end{pmatrix}. \quad (2)$$

The matrix that appears here as an effective Hamiltonian,  $H_{\text{eff}}$ , is clearly non-Hermitian, and embodies the well-known concept of the  $\mathcal{PT}$ -symmetry breaking transition [18, 20–27, 29, 30], as is shown in Fig. 2. Solving the characteristic polynomial for the eigenvalues  $k$  of this effective Hamiltonian,

$$k = \pm \sqrt{\omega^2 - m^2} \quad (3)$$

we can see that if  $\omega$  is a real number, the solution for  $k$  can alternatively be real, or imaginary. This embodies the regions of respectively unbroken (Fig. 2(a)) and broken  $\mathcal{PT}$ -symmetry (Fig. 2(c)), with an exceptional point (EP) occurring for  $|\omega| = m$  (Fig. 2(b)) [15, 23, 27, 28, 41, 42]. Additionally, since  $H_{\text{eff}}$  is non-Hermitian, its eigenvectors are generally non-orthogonal.

This establishes the principle that we employ to harness quantum evolution in a resource-efficient manner for quantum simulation: we now let the laboratory time coordinate represent the spatial coordinate of Eq. 2, such

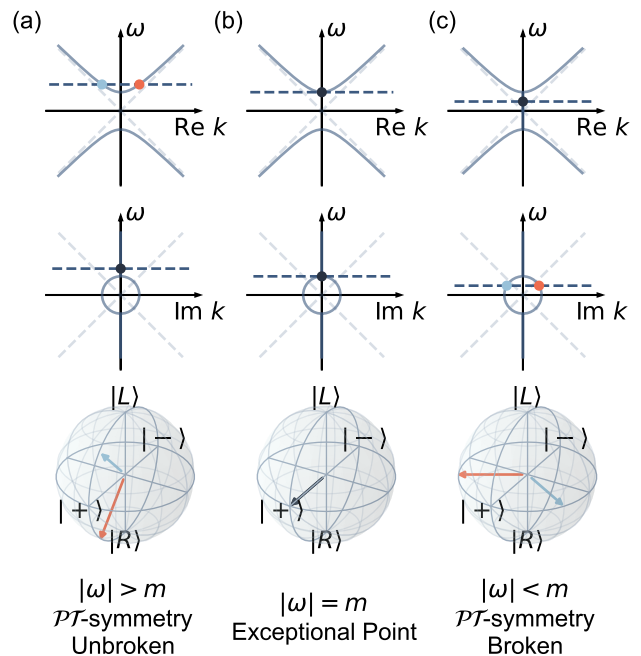


FIG. 2.  **$\mathcal{PT}$ -symmetry.** The parameter space is categorized by the status of the  $\mathcal{PT}$ -symmetry. In each case, the horizontal dashed line represents the eigenenergy and the arrows represent the eigenvectors of  $H_{\text{eff}}$ . (a) When  $|\omega| > m$ , the  $\mathcal{PT}$ -symmetry is unbroken. The eigenmomenta of  $H_{\text{eff}}$  are a pair of real numbers with opposite signs. (b) When  $|\omega| = m$ , the system is at the exceptional point with the eigenmomenta coalescing to 0. (c) When  $|\omega| < m$ , the  $\mathcal{PT}$ -symmetry is broken. The eigenmomenta of  $H_{\text{eff}}$  are a pair of purely imaginary numbers with opposite signs.

that the real-time evolution of a qubit captures the spatial solution of a chosen problem. We refer to this principle as the *qubit hologram* because the qubit encodes the wavefront of the spatial solution. In general, we are interested in the scattering or bound states of a given potential  $V(x)$ , which can now be obtained from the time evolution under,

$$H(t) = \begin{pmatrix} E - V(t) & -m \\ m & -E + V(t) \end{pmatrix}, \quad (4)$$

where we have replaced  $\omega$  with  $E$  to emphasize it now represents the eigenenergy of the problem.

*Example 1: Scattering phase shifts*—The problem of solving the cross section of an elastic neutron scattering off an atomic nucleus described by an optical potential can be reduced to a 1D problem through partial wave decomposition (Fig. 3(a)) [43], which gives a differential equation for the radial wave function  $u_{lj}(r)$  for the orbital angular momentum quantum number  $l$  and total angular momentum number  $j$ ,

$$u_{lj}''(r) + \left[ k^2 - \frac{2m}{\hbar^2} V_{lj}(r) - \frac{l(l+1)}{r^2} \right] u_{lj}(r) = 0, \quad (5)$$

where  $V_{lj}(r)$  is given by the global optical model CH89

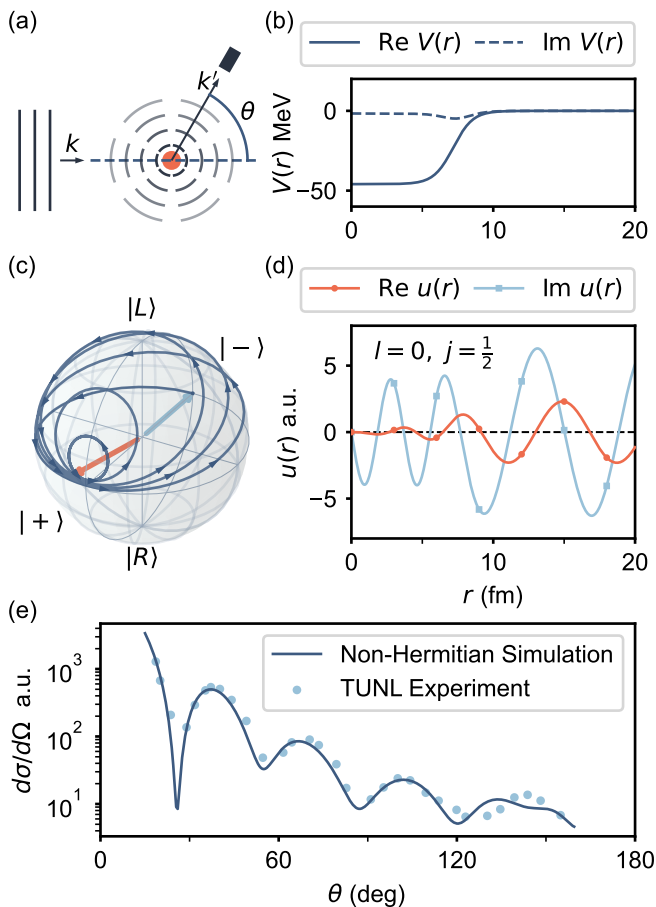


FIG. 3. **Simulating scattering phase shifts with qubit dynamics.** (a) The scattering of a neutron in plane wave state given by wavevector  $\mathbf{k}$  scattering off of a nucleus can be expressed in terms of the radial wavefunction for the scattering state  $u_{lj}(r)$ . By mapping the radial wavefunction to the components of a spinor describing a qubit, the spatial solution  $u_{lj}(r)$  of the scattering problem corresponds to the time evolution  $|\psi\rangle(t)$ . (b) The potential function  $V_{lj}(r)$  for  $^{208}\text{Pb}$  atomic nucleus given by CH89. (c) The trajectory on the Bloch sphere. The vectors have been normalized to make them stay on the Bloch sphere. (d) The scattering wavefunction for the lowest partial wave channel ( $l = 0, j = \frac{1}{2}$ ). (e) Unpolarized differential cross section calculated from the non-Hermitian Hamiltonian compared to the experimental result.

[44]. We will show how this differential equation can be mapped onto the temporal dynamics of a qubit evolving in a time-dependent Hamiltonian. For this purpose we find it convenient to work in the  $|\pm\rangle$  basis. The time evolution of a qubit state  $|\psi\rangle$  expressed in the basis  $|\psi\rangle = \alpha|+\rangle + \beta|-\rangle$ , is given by a Hamiltonian  $H$ , which can be represented as a  $2 \times 2$  matrix.

By introducing a transformation between the spatial and time coordinates  $r = vt$ , where  $v$  is a scaling parameter, we relate the qubit state  $|\psi\rangle$  with the solution of

the wavefunction,  $u_{lj}(r)$  by writing,

$$\alpha(t) = \sqrt{2}u_{lj}(r), \quad (6)$$

$$\beta(t) = i\partial_r u_{lj}(r)/(\sqrt{2}m), \quad (7)$$

such that the expansion coefficients  $\alpha(t), \beta(t)$  encode the wave function and its derivative.

To capture the solution to the differential equation (5) as temporal dynamics, we need the expansion coefficients to obey the differential equations,

$$i\partial_t \alpha(t) = 2vm\beta(t), \quad (8)$$

$$i\partial_t \beta(t) = v(E - V_{\text{tot}}(vt))\alpha(t), \quad (9)$$

where

$$V_{\text{tot}}(r) = V_{lj}(r) + \frac{\hbar^2}{2m} \frac{l(l+1)}{r^2}, \quad (10)$$

is the total potential including the centrifugal term. The evolution described above can be implemented by a Hamiltonian written as

$$H_{\text{eff}}(t) = v \begin{pmatrix} E - V_{\text{tot}}(vt) & 2m \\ & \end{pmatrix}, \quad (11)$$

which is non-Hermitian. A non-Hermitian Hamiltonian such as Eq. 11 can be obtained, for example, through the evolution of a dissipative qubit where post-selection is used to eliminate quantum jumps [18, 19, 45, 46]. Another approach for synthesizing non-Hermitian dynamics is based on Hamiltonian dilation. However, this method requires additional computational resources.

Figure 3 displays a specific example where the evolution of a qubit is used to solve for the first partial wave channel ( $l = 0, j = 1/2$ ) scattering of a neutron off of a  $^{208}\text{Pb}$  nucleus. Figure 3(b) displays the potential of the nucleus, where the imaginary part of the potential corresponds to the process of neutron capture. We calculate the time evolution of a qubit evolving under Eq. 11 using QuTiP [47, 48]. Figure 3(c) displays the resulting time evolution of the qubit, initialized in the state  $|-\rangle$ , from which we determine the partial wave solution  $u_{lj}(r)$  (Fig. 3(d)). By comparing the final phase to the solution for the free particle, we can determine the scattering phase shift and the scattering cross section [43]. By evaluating a series of these partial waves, we can sum up their scattering contributions and compare the result to the experimental data [44] as shown in Fig. 3(e).

*Example 2: Majorana zero mode*— In addition to scattering states which allow a continuum of eigenenergy values, our formalism also applies to bound states. In particular, topological bound states are a class of bound states with rich physics. We'll show how our method is able to solve for such states, and how the  $\mathcal{PT}$ -symmetry transition signals a topological phase transition. Here we demonstrate a Majorana zero mode as an edge state of the Kitaev chain which is a simplified model of a

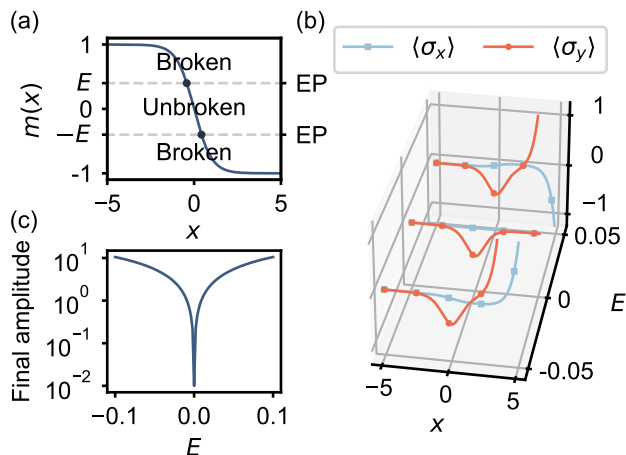


FIG. 4. **Majorana zero mode.** (a) The spatially dependent mass  $m(x)$ . When  $|m| > |E|$  ( $|m| < |E|$ ) the system is in the  $\mathcal{PT}$ -symmetric broken (unbroken) phase. When  $m = \pm E$  the system is at the EP. (b) The wavefunction of the Majorana zero mode given by the  $\langle \sigma_x \rangle, \langle \sigma_y \rangle$  Bloch components for three different trial energy eigenvalues  $E$ . The trace for  $\langle \sigma_z \rangle = 0$  is unshown. (c) The final amplitude of the quantum state at  $x = 5$ .

topological superconductor [36]. The realistic version has been experimentally demonstrated in semiconducting nanowires in proximity to superconductors [49–52].

The band structure of a condensed matter system describes the behavior of its excitations. Under perturbations, the band structure can be deformed. For a gapped system such as an insulator, a finite gap separates the bands. For small perturbations, this gap cannot be closed. As a result, for insulators, continuous perturbation induces continuous deformation of the band structure, yet these deformations are topologically equivalent. If a region of the normal band structure is connected to a region of inverted band structure, indicated by negative gap energy, the gap is forced to close giving rise to a bound state. This gap closure is topologically protected, resulting in topologically protected bound states. In the case of a topological superconductor, the edge state is a Majorana zero mode.

The two topological phases that enclose the bound state correspond to regions of effective positive and negative mass, which we model as  $m(x) = -\tanh(x)$ . To calculate the bound states of this system, we again replace the spatial coordinate with the temporal coordinate such that the bound state appears in the time evolution of the effective Hamiltonian,

$$H_{\text{eff}}(t) = \begin{pmatrix} E & -m(t) \\ m(t) & -E \end{pmatrix}, \quad (12)$$

where  $m(t)$  is the mass of the excitation that switches sign from +1 to -1 during the evolution (Fig. 4(a)).  $E$  is the trial solution to the eigenvalue problem.

For the eigenvalue problem of bound states, the

method works as a variational eigensolver. The key observation is the wave function of a bound state is an evanescent wave outside of the interface. This physical constraint guarantees its amplitude to vanish at sufficiently large distances. In our case, we focus on the regime with  $E \ll m(t = 0)$ , where the Hamiltonian is dominated by the  $\sigma_y$  component. We initialize the qubit in the  $|y-\rangle = \frac{1}{\sqrt{2}}(|L\rangle - i|R\rangle)$  eigenstate of the non-Hermitian Hamiltonian when  $m = 1$ , featuring an exponential gain behavior. Next, we let the system evolve under the non-Hermitian Hamiltonian to obtain the corresponding trial wavefunction (Fig. 4(b)). We repeat the process with various trial eigenenergies and try to make the final state converge to an exponentially decaying state for the non-Hermitian Hamiltonian when  $m = -1$ . Figure 4(c) displays the final amplitude (at  $x = 5$ ) as a function of  $E$  showing that the bound state occurs at  $E = 0$  as expected.

Now, we explain why  $\mathcal{PT}$ -symmetric physics is important here. For a given  $E$  there are typically two classical turning points, which are the EPs of  $H_{\text{eff}}$ . The EPs separate regions of broken and unbroken  $\mathcal{PT}$ -symmetry corresponding respectively to exponential or oscillatory solutions. This is similar to what one encounters in the study of bound states in elementary quantum mechanics. Here, with no external potential, the choice of  $E$  specifies the EPs, and in particular when  $E \rightarrow 0$  the two EPs merge. The merging of the two EPs corresponds to the topological phase transition that produces the Majorana bound state.

We have so far discussed two examples that show how the non-Hermitian time evolution of a qubit can be used to emulate the spatial solutions of scattering and bound state systems. This is the basis of the qubit hologram; in higher than one dimension the quantum state in the bulk can be encoded in the time evolution of the edge qubit hologram. Additionally, the qubit hologram will inherit the  $\mathcal{P}$  symmetry from the bulk system as  $\mathcal{PT}$ -symmetry. We demonstrate the concept with a spin-1/2 particle moving in three dimensions governed by the Dirac Hamiltonian

$$H(\mathbf{k}) = \begin{pmatrix} -\boldsymbol{\sigma} \cdot \mathbf{k} & m \\ m & \boldsymbol{\sigma} \cdot \mathbf{k} \end{pmatrix}, \quad (13)$$

which is a  $4 \times 4$  matrix written in the block form. We choose to work in the momentum representation for the simplicity of the ensuing expressions.  $\boldsymbol{\sigma}$  represents the Pauli matrices and  $\mathbf{k}$  represents the momentum. The Dirac Hamiltonian conserves parity

$$\mathcal{P}^{-1}H(\mathbf{k})\mathcal{P} = H(-\mathbf{k}), \quad \mathcal{P} = -\mathcal{P}^{-1} = i \begin{pmatrix} & I \\ I & \end{pmatrix}, \quad (14)$$

where we have included the prefactor  $i$  in  $\mathcal{P}$  to make it comply with the parity of multi-particle wavefunctions [53].  $\mathcal{P}$  can be decomposed into three separate mirror

reflection operators

$$\mathcal{P} = M_x M_y M_z, \quad M_j = M_j^{-1} = \begin{pmatrix} & \sigma_j \\ \sigma_j & \end{pmatrix}, \quad (15)$$

where  $j = x, y, z$ . The qubit hologram allows us to treat the  $z$  coordinate as the effective time axis, which yields the effective Hamiltonian,

$$H_{\text{eff}}(\omega, k_x, k_y) = \begin{pmatrix} \omega\sigma_z + i(k_x\sigma_y - k_y\sigma_x) & -m\sigma_z \\ m\sigma_z & -\omega\sigma_z + i(k_x\sigma_y - k_y\sigma_x) \end{pmatrix}. \quad (16)$$

Since the initial system of the Dirac Hamiltonian is parity symmetric, the qubit hologram (16) now obeys  $\mathcal{PT}$ -symmetry.

$$\mathcal{P}_{\text{eff}} \mathcal{T}_{\text{eff}} H_{\text{eff}}(\omega, k_x, k_y) \mathcal{P}_{\text{eff}} \mathcal{T}_{\text{eff}} = H_{\text{eff}}(\omega, -k_x, -k_y), \quad (17)$$

where the time reversal and the parity operations are characterized by

$$\mathcal{T}_{\text{eff}} = M_z = \begin{pmatrix} & \sigma_z \\ \sigma_z & \end{pmatrix}, \quad \mathcal{P}_{\text{eff}} = M_x M_y = i \begin{pmatrix} \sigma_z & \\ & \sigma_z \end{pmatrix}, \quad (18)$$

respectively. We note two subtleties regarding this representation: (i) Here,  $\mathcal{T}_{\text{eff}}$  is a unitary operator (inherited from  $M_z$ ) rather than an anti-unitary operator which involves complex conjugation and is typically associated with time reversal. (ii) The  $\mathcal{P}_{\text{eff}} \mathcal{T}_{\text{eff}}$  operator transforms the original Hamiltonian with momentum  $(k_x, k_y)$  into a different Hamiltonian with spatially inverted momentum  $(-k_x, -k_y)$ . For this reason, the  $\mathcal{PT}$ -symmetry here appears to be different than what is typically encountered in the literature. The second subtlety can be addressed by considering the coordinate representation of the Hamiltonian or an extended momentum representation containing both  $(k_x, k_y)$  and  $(-k_x, -k_y)$ . Furthermore, by redefining the complex numbers and the associated complex conjugation of the matrix elements, the anti-unitary nature of  $\mathcal{T}_{\text{eff}}$  can be restored.

*Conclusion*— Many of the leading technologies for quantum processors consist of a fixed number of qubits that evolve in real-time with an evolution that can be characterized by a sequence of single and multi-qubit gates and ongoing effects of decoherence. In contrast, for applications of quantum simulation, we are typically interested in static properties with spatial structure, such as bound states, scattering cross-sections, and spatial correlations. Therefore, to effectively utilize a quantum simulator, it is desirable to understand how the time axis can be used to capture spatial structure. To achieve this, we have introduced a proper space-to-time transform—the qubit hologram—that is able to assign one of the spatial dimensions a new meaning of an effective time axis.

In nature, many physical systems can be described by Hamiltonians that respect  $\mathcal{P}$  symmetry. Examples include field theories such as Quantum Chromodynamics

and crystals with inversion symmetry such as graphene. As we have seen, the eigenvalue problem for systems with  $\mathcal{P}$  symmetry will map on to  $\mathcal{PT}$ -symmetric dynamics of the system's qubit hologram. Here, the real-space solutions corresponding to traveling waves, evanescent waves, and particles at rest map onto the familiar unbroken region, broken region, and exceptional points of  $\mathcal{PT}$ -symmetry.

We are grateful to Yogesh Joglekar, Carl Bender, Saori Pastore, Maria Piarulli, Alexander Seidel, Weijian Chen, and Maryam Abbasi for helpful discussions. This research was supported by NSF Grant No. PHY-1752844 (CAREER), AFOSR MURI Grant No. FA9550-21-1-0202, and ONR Grant No. N00014-21-1-2630.

- 
- [1] R. P. Feynman, Simulating physics with computers, *International Journal of Theoretical Physics* **21**, 467 (1982).
  - [2] D. P. DiVincenzo, Two-bit gates are universal for quantum computation, *Physical Review A* **51**, 1015 (1995), arXiv:9407022 [cond-mat].
  - [3] A. Barenco, C. H. Bennett, R. Cleve, D. P. DiVincenzo, N. Margolus, P. Shor, T. Sleator, J. A. Smolin, and H. Weinfurter, Elementary gates for quantum computation, *Physical Review A* **52**, 3457 (1995).
  - [4] F. Arute, K. Arya, R. Babbush, D. Bacon, J. C. Bardin, R. Barends, R. Biswas, S. Boixo, F. G. Brandao, D. A. Buell, B. Burkett, Y. Chen, Z. Chen, B. Chiaro, R. Collins, W. Courtney, A. Dunsworth, E. Farhi, B. Foxen, A. Fowler, C. Gidney, M. Giustina, R. Graff, K. Guerin, S. Habegger, M. P. Harrigan, M. J. Hartmann, A. Ho, M. Hoffmann, T. Huang, T. S. Humble, S. V. Isakov, E. Jeffrey, Z. Jiang, D. Kafri, K. Kechedzhi, J. Kelly, P. V. Klimov, S. Knysh, A. Korotkov, F. Kostritsa, D. Landhuis, M. Lindmark, E. Lucero, D. Lyakh, S. Mandrà, J. R. McClean, M. McEwen, A. Megrant, X. Mi, K. Michielsen, M. Mohseni, J. Mutus, O. Naaman, M. Neeley, C. Neill, M. Y. Niu, E. Ostby, A. Petukhov, J. C. Platt, C. Quintana, E. G. Rieffel, P. Roushan, N. C. Rubin, D. Sank, K. J. Satzinger, V. Smelyanskiy, K. J. Sung, M. D. Trevithick, A. Vainsencher, B. Villalonga, T. White, Z. J. Yao, P. Yeh, A. Zalcman, H. Neven, and J. M. Martinis, Quantum supremacy using a programmable superconducting processor, *Nature* **574**, 505 (2019).
  - [5] L. K. Grover, Quantum mechanics helps in searching for a needle in a haystack, *Physical Review Letters* **79**, 325 (1997).
  - [6] J. Preskill, Quantum Computing in the NISQ era and beyond, *Quantum* **2**, 79 (2018), arXiv:1801.00862.
  - [7] H. P. Breuer and F. Petruccione, *The Theory of Open Quantum Systems*, Vol. 9780199213900 (Oxford University Press, Oxford, 2007).
  - [8] C. P. Koch, Controlling open quantum systems: Tools, achievements, and limitations, *Journal of Physics Condensed Matter* **28**, 10.1088/0953-8984/28/21/213001 (2016), arXiv:1603.04417.
  - [9] E. Kapit, The upside of noise: engineered dissipation as

- a resource in superconducting circuits, *Quantum Science and Technology* **2**, 033002 (2017).
- [10] S. Diehl, A. Micheli, A. Kantian, B. Kraus, H. P. Büchler, and P. Zoller, Quantum states and phases in driven open quantum systems with cold atoms, *Nature Physics* **4**, 878 (2008), arXiv:0803.1482.
  - [11] S. Shankar, M. Hatridge, Z. Leghtas, K. M. Sliwa, A. Narla, U. Vool, S. M. Girvin, L. Frunzio, M. Mirrahimi, and M. H. Devoret, Autonomously stabilized entanglement between two superconducting quantum bits, *Nature* **504**, 419 (2013).
  - [12] P. M. Harrington, E. Mueller, and K. Murch, Engineered dissipation for quantum information science (2022), arXiv:2202.05280.
  - [13] K. W. Murch, U. Vool, D. Zhou, S. J. Weber, S. M. Girvin, and I. Siddiqi, Cavity-assisted quantum bath engineering, *Physical Review Letters* **109**, 1 (2012), arXiv:1207.0053.
  - [14] P. M. Harrington, M. Naghiloo, D. Tan, and K. W. Murch, Bath engineering of a fluorescing artificial atom with a photonic crystal, *Physical Review A* **99**, 1 (2019), arXiv:1812.04205.
  - [15] W. Chen, S. K. Özdemir, G. Zhao, J. Wiersig, and L. Yang, Exceptional points enhance sensing in an optical microcavity, *Nature* **548**, 192 (2017).
  - [16] X. Mi, M. Ippoliti, C. Quintana, A. Greene, Z. Chen, J. Gross, F. Arute, K. Arya, J. Atalaya, R. Babush, J. C. Bardin, J. Basso, A. Bengtsson, A. Bilmes, A. Bourassa, L. Brill, M. Broughton, B. B. Buckley, D. A. Buell, B. Burkett, N. Bushnell, B. Chiaro, R. Collins, W. Courtney, D. Debroy, S. Demura, A. R. Derk, A. Dunsworth, D. Eppens, C. Erickson, E. Farhi, A. G. Fowler, B. Foxen, C. Gidney, M. Giustina, M. P. Harrigan, S. D. Harrington, J. Hilton, A. Ho, S. Hong, T. Huang, A. Huff, W. J. Huggins, L. B. Ioffe, S. V. Isakov, J. Iveland, E. Jeffrey, Z. Jiang, C. Jones, D. Kafri, T. Khattar, S. Kim, A. Kitaev, P. V. Klimov, A. N. Korotkov, F. Kostritsa, D. Landhuis, P. Laptev, J. Lee, K. Lee, A. Locharla, E. Lucero, O. Martin, J. R. McClean, T. McCourt, M. McEwen, K. C. Miao, M. Mohseni, S. Montazeri, W. Mruczkiewicz, O. Naaman, M. Neeley, C. Neill, M. Newman, M. Y. Niu, T. E. O'Brien, A. Opremcak, E. Ostby, B. Pato, A. Petukhov, N. C. Rubin, D. Sank, K. J. Satzinger, V. Shvarts, Y. Su, D. Strain, M. Szalay, M. D. Trevithick, B. Valllonga, T. White, Z. J. Yao, P. Yeh, J. Yoo, A. Zalcman, H. Neven, S. Boixo, V. Smelyanskiy, A. Megrant, J. Kelly, Y. Chen, S. L. Sondhi, R. Moessner, K. Kechedzhi, V. Khemani, and P. Roushan, Time-crystalline eigenstate order on a quantum processor., *Nature* **601**, 531 (2022).
  - [17] J. F. Poyatos, J. I. Cirac, and P. Zoller, Quantum reservoir engineering with laser cooled trapped ions, *Physical Review Letters* **77**, 4728 (1996).
  - [18] M. Naghiloo, M. Abbasi, Y. N. Joglekar, and K. W. Murch, Quantum state tomography across the exceptional point in a single dissipative qubit, *Nature Physics* **15**, 1232 (2019).
  - [19] M. Abbasi, W. Chen, M. Naghiloo, Y. N. Joglekar, and K. W. Murch, Topological quantum state control through exceptional-point proximity, *Physical Review Letters* **128**, 10.1103/physrevlett.128.160401 (2022).
  - [20] Y. Wu, W. Liu, J. Geng, X. Song, X. Ye, C. K. Duan, X. Rong, and J. Du, Observation of parity-time symmetry breaking in a single-spin system, *Science* **364**, 878 (2019), arXiv:1812.05226.
  - [21] C. E. Rüter, K. G. Makris, R. El-Ganainy, D. N. Christodoulides, M. Segev, and D. Kip, Observation of parity-time symmetry in optics, *Nature Physics* **6**, 192 (2010).
  - [22] A. Regensburger, C. Bersch, M. A. Miri, G. Onishchukov, D. N. Christodoulides, and U. Peschel, Parity-time synthetic photonic lattices, *Nature* **488**, 167 (2012).
  - [23] B. Peng, S. K. Özdemir, S. Rotter, H. Yilmaz, M. Liertzer, F. Monifi, C. M. Bender, F. Nori, and L. Yang, Loss-induced suppression and revival of lasing, *Science* **346**, 328 (2014).
  - [24] R. El-Ganainy, K. G. Makris, M. Khajavikhan, Z. H. Musslimani, S. Rotter, and D. N. Christodoulides, Non-Hermitian physics and PT symmetry, *Nature Physics* **14**, 11 (2018).
  - [25] K. G. Makris, R. El-Ganainy, D. N. Christodoulides, and Z. H. Musslimani, Beam dynamics in PT symmetric optical lattices, *Physical Review Letters* **100**, 1 (2008).
  - [26] A. Guo, G. J. Salamo, D. Duchesne, R. Morandotti, M. Volatier-Ravat, V. Aimez, G. A. Siviloglou, and D. N. Christodoulides, Observation of PT-symmetry breaking in complex optical potentials, *Physical Review Letters* **103**, 1 (2009).
  - [27] L. Feng, Y. L. Xu, W. S. Fegadolli, M. H. Lu, J. E. Oliveira, V. R. Almeida, Y. F. Chen, and A. Scherer, Experimental demonstration of a unidirectional reflectionless parity-time metamaterial at optical frequencies, *Nature Materials* **12**, 108 (2013).
  - [28] H. Hodaei, A. U. Hassan, S. Wittek, H. Garcia-Gracia, R. El-Ganainy, D. N. Christodoulides, and M. Khajavikhan, Enhanced sensitivity at higher-order exceptional points, *Nature* **548**, 187 (2017).
  - [29] C. M. Bender and S. Boettcher, Real spectra in non-hermitian hamiltonians having PT symmetry, *Physical Review Letters* **80**, 5243 (1998), arXiv:9712001 [physics].
  - [30] C. M. Bender, Making sense of non-Hermitian Hamiltonians, *Reports on Progress in Physics* **70**, 947 (2007), arXiv:0703096 [hep-th].
  - [31] L. Xiao, T. Deng, K. Wang, G. Zhu, Z. Wang, W. Yi, and P. Xue, Non-hermitian bulk-boundary correspondence in quantum dynamics, *Nature Physics* **16**, 10.1038/s41567-020-0836-6 (2020).
  - [32] S. Yao and Z. Wang, Edge States and Topological Invariants of Non-Hermitian Systems, *Physical Review Letters* **121**, 86803 (2018).
  - [33] F. K. Kunst, E. Edvardsson, J. C. Budich, and E. J. Bergholtz, Biorthogonal Bulk-Boundary Correspondence in Non-Hermitian Systems, *Physical Review Letters* **121**, 26808 (2018).
  - [34] S. Weidemann, M. Kremer, T. Helbig, T. Hofmann, A. Stegmaier, M. Greiter, R. Thomale, and A. Szameit, Topological funneling of light, *Science* **368**, 311 (2020).
  - [35] Z. Gong, Y. Ashida, K. Kawabata, K. Takasan, S. Higashikawa, and M. Ueda, Topological Phases of Non-Hermitian Systems, *Physical Review X* **8**, 31079 (2018), arXiv:1802.07964.
  - [36] A. Y. Kitaev, Unpaired Majorana fermions in quantum wires, *Physics-Uspekhi* **44**, 131 (2001), arXiv:0010440 [cond-mat].
  - [37] X. L. Qi and S. C. Zhang, Topological insulators and superconductors, *Reviews of Modern Physics* **83**, 10.1103/RevModPhys.83.1057 (2011), arXiv:1008.2026.

- [38] M. Z. Hasan and C. L. Kane, Colloquium: Topological insulators, *Reviews of Modern Physics* **82**, 3045 (2010).
- [39] L. Fu and C. L. Kane, Superconducting proximity effect and majorana fermions at the surface of a topological insulator, *Physical Review Letters* **100**, 1 (2008), arXiv:0707.1692.
- [40] S. R. Elliott and M. Franz, Colloquium: Majorana fermions in nuclear, particle, and solid-state physics, *Reviews of Modern Physics* **87**, 10.1103/RevModPhys.87.137 (2015), arXiv:1403.4976.
- [41] W. D. Heiss, The physics of exceptional points, *Journal of Physics A: Mathematical and Theoretical* **45**, 444016 (2012).
- [42] M.-A. Miri and A. Alù, Exceptional points in optics and photonics, *Science* **363**, 10.1126/science.aar7709 (2019).
- [43] C. J. Joachain, *Quantum collision theory* (North-Holland, Netherlands, 1975) pp. 490–502.
- [44] R. Varner, W. Thompson, T. McAbee, E. Ludwig, and T. Clegg, A global nucleon optical model potential, *Physics Reports* **201**, 57 (1991).
- [45] J. Dalibard, Y. Castin, and K. Mølmer, Wave-function approach to dissipative processes in quantum optics, *Physical Review Letters* **68**, 580 (1992).
- [46] M. B. Plenio and P. L. Knight, The quantum-jump approach to dissipative dynamics in quantum optics, *Reviews of Modern Physics* **70**, 101 (1998), arXiv:9702007 [quant-ph].
- [47] J. R. Johansson, P. D. Nation, and F. Nori, QuTiP: An open-source Python framework for the dynamics of open quantum systems, *Computer Physics Communications* **183**, 1760 (2012), arXiv:1110.0573.
- [48] J. R. Johansson, P. D. Nation, and F. Nori, QuTiP 2: A Python framework for the dynamics of open quantum systems, *Computer Physics Communications* **184**, 1234 (2013), arXiv:1211.6518.
- [49] V. Mourik, K. Zuo, S. M. Frolov, S. R. Plissard, E. P. Bakkers, and L. P. Kouwenhoven, Signatures of Majorana Fermions in Topological Superconductor Nanowires, *Science* **336**, 1003 (2012).
- [50] A. Das, Y. Ronen, Y. Most, Y. Oreg, M. Heiblum, and H. Shtrikman, Zero-bias peaks and splitting in an Al-InAs nanowire topological superconductor as a signature of Majorana fermions, *Nature Physics* **8**, 887 (2012).
- [51] M. T. Deng, S. Vaitiekenas, E. B. Hansen, J. Danon, M. Leijnse, K. Flensberg, J. Nygård, P. Krogstrup, and C. M. Marcus, Majorana bound state in a coupled quantum-dot hybrid-nanowire system, *Science* **354**, 1557 (2016), arXiv:1612.07989.
- [52] R. M. Lutchyn, E. P. Bakkers, L. P. Kouwenhoven, P. Krogstrup, C. M. Marcus, and Y. Oreg, Majorana zero modes in superconductor-semiconductor heterostructures, *Nature Reviews Materials* **3**, 52 (2018).
- [53] M. Srednicki, *Quantum Field Theory* (Cambridge University Press, 2007).

## Supplemental Material

In the supplemental material, we explain the calculation of the neutron scattering cross section.

### SCATTERING CROSS SECTION

The asymptotic scattering wave function for angular momentum  $l$  is written as

$$u_l(r) = Cr[\cos \delta_l j_l(kr) - \sin \delta_l n_l(kr)], \quad (19)$$

where  $j_l(x)$  and  $n_l(x)$  are the spherical Bessel and Neumann functions, respectively.  $C$  is the normalization constant,  $\delta_l$  is the scattering phase shift and  $k$  is the wave number. Here,  $r$  should be sufficiently larger than the radius of the atomic nucleus. In order to extract  $\delta_l$  from the wave function, we choose two points  $R_1$  and  $R_2$  to obtain

$$G = \frac{R_2 u_l(R_1)}{R_1 u_l(R_2)}, \quad \tan \delta_l = \frac{j_l(kR_1) - G j_l(kR_2)}{n_l(kR_1) - G n_l(kR_2)}. \quad (20)$$

Since the neutron is a spin-1/2 particle, the corresponding scattering phase shift  $\delta_{lj}$  is labeled by an extra  $j = l \pm \frac{1}{2}$  (or as  $j = \pm$  for convenience) denoting the total angular momentum of the system under spin-orbital coupling. In our calculation, we use  $R_1 = 19.98$  fm and  $R_2 = 20.00$  fm, while the radius of the  $^{208}\text{Pb}$  nucleus is around 7.18 fm. For simplicity, we have ignored the change of reference frame and treated the atomic nucleus of  $^{208}\text{Pb}$  as stationary. After obtaining the scattering phase shift, we can calculate the scattering amplitudes

$$f(k, \theta) = \frac{1}{2ik} \sum_{l=0}^{\infty} [(l+1)(e^{2i\delta_{l+}} - 1) + l(e^{2i\delta_{l-}} - 1)] P_l(\cos \theta), \quad (21)$$

$$g(k, \theta) = \frac{\sin \theta}{2k} \sum_{l=0}^{\infty} (e^{2i\delta_{l+}} - e^{2i\delta_{l-}}) P'_l(\cos \theta), \quad (22)$$

where  $P_l$  ( $P'_l$ ) are the (derivative of) Legendre polynomials. In the summation, we choose the cutoff angular momentum to be  $l = 12$ . The unpolarized cross section is given by

$$\left(\frac{d\sigma}{d\Omega}\right)_{\text{unpol}} = |f|^2 + |g|^2, \quad (23)$$

which can be compared with the experimental data.